Electronic Supporting Information

Study of the complex formation between the $[Cu(bpca)]^+$ secondary building unit and the aromatic *N*-donors 2,3,5,6-tetra(2-pyridyl)pyrazine (tppz) and 1,3-bis(4-pyridyl)propane (bpp)†

Eloisa de Oliveira Ribeiro,[a] Nathália Rodrigues de Campos,[a] Antônio Carlos Doriguetto,[a] Wdeson Pereira Barros,[b] Marcos Antônio Ribeiro,[c] Elgte E. B. De Paula[d], Humberto Osório Stumpf,[e] Francesc Lloret,[f] Miguel Julve,[f] and Maria Vanda Marinho.[a*]

[a]Instituto de Química, Universidade Federal de Alfenas, Alfenas, MG 37130-000, Brazil. *E-mail: mvmarinho09@gmail.com

[b]Instituto de Química, Universidade Estadual de Campinas, Departamento de Química Inorgânica, Campinas, SP 13083-970, Brazil

[c]Departamento de Química, Universidade Federal do Espírito Santo,Vitória, ES 29075-910, Brazil

[d]Instituto Federal de Educação, Ciência e Tecnologia do Sul de Minas Gerais, Pouso Alegre, MG 37550-000, Brazil.

[e]Departamento de Química – ICEx, Universidade Federal de Minas Gerais, Belo Horizonte, MG 31270-901, Brazil.

[f]Instituto de Ciencia Molecular/Departament de Quimica Inorgànica, Universitat de València, C/ Catedrático José Beltrán 2, 46980 Paterna, València, Spain.

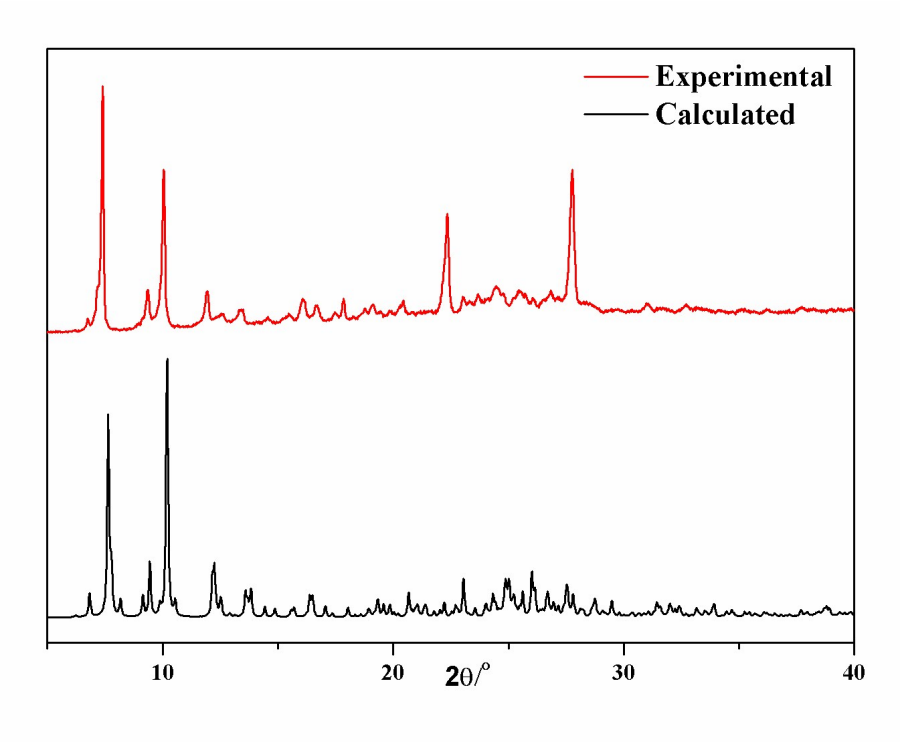

Figure S1 Experimental (red) and calculated (black) PXRD patterns of **1**.

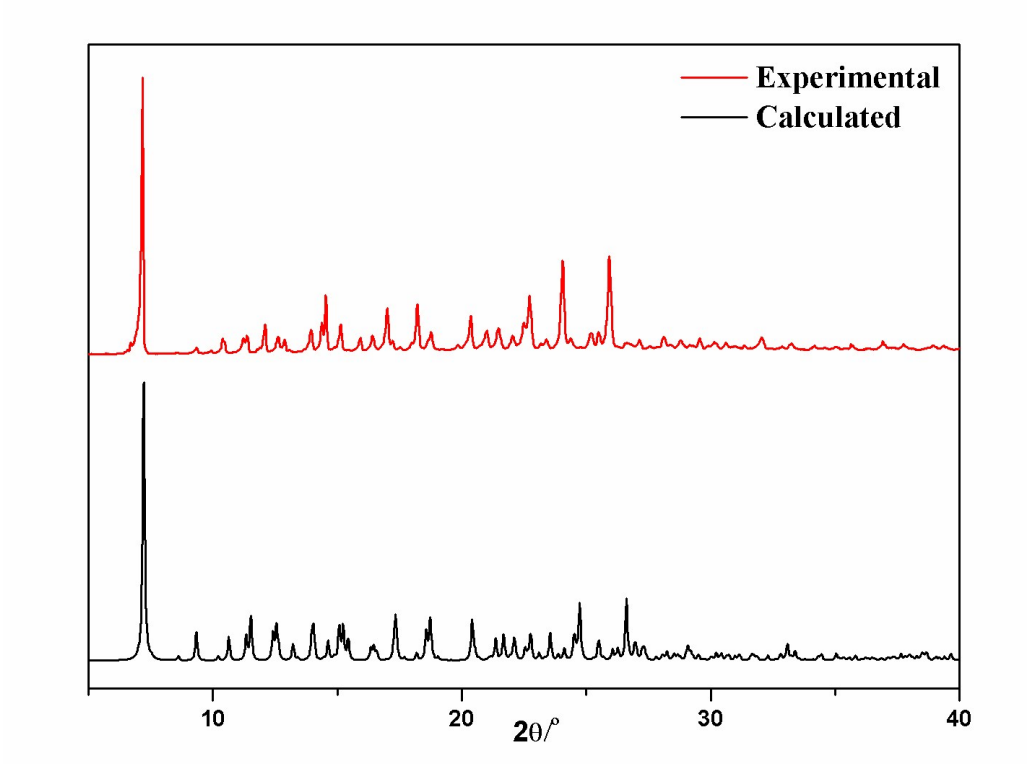

Figure S2 Experimental (red) and calculated (black) PXRD patterns of **2**.

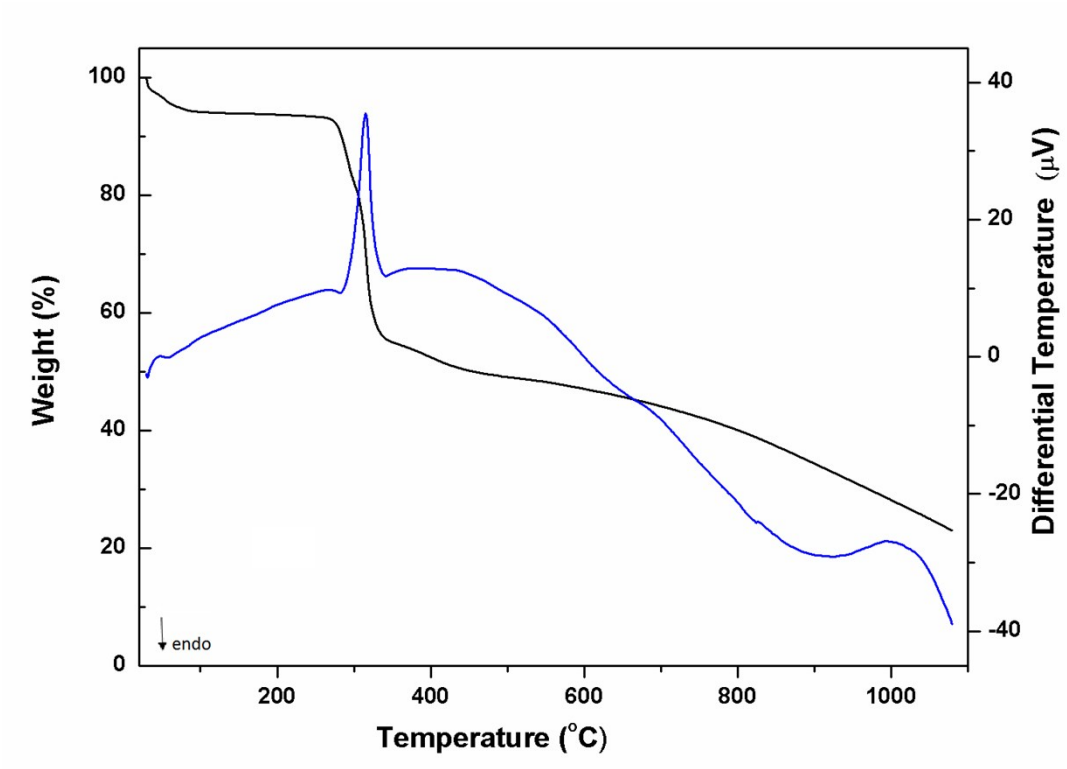

(a)

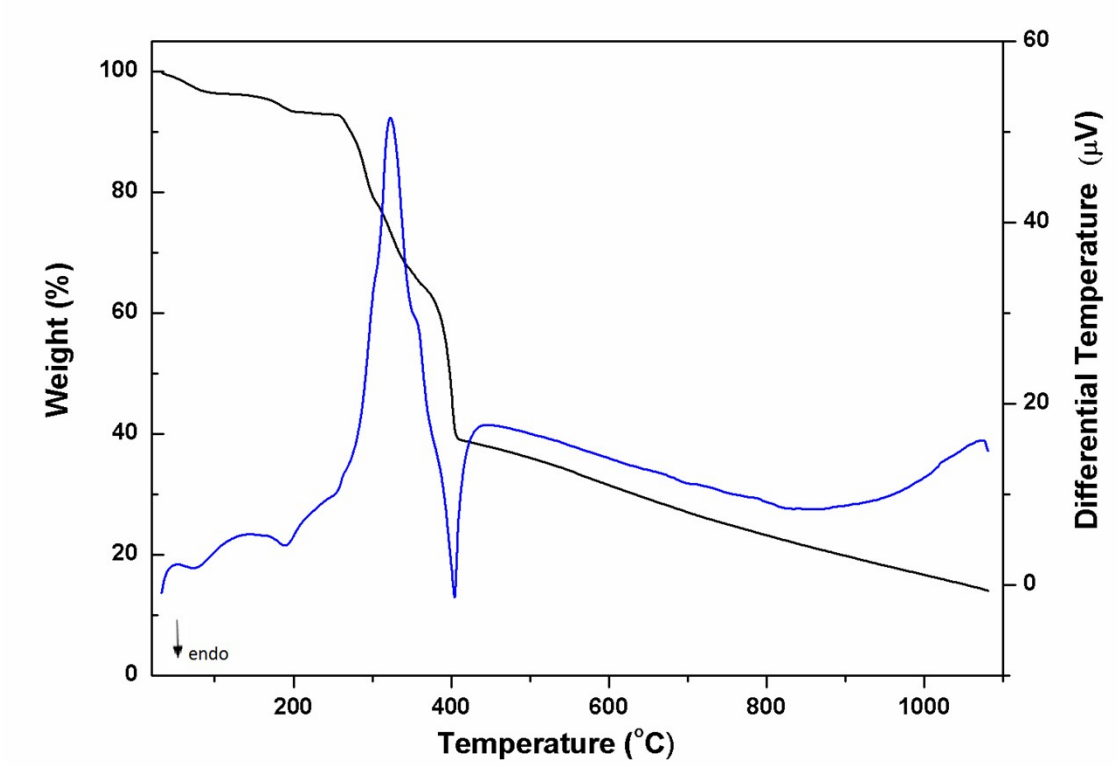

(b)

Figure S3 TG and DTA curves for (a) **1** and (b) **2**, respectively.

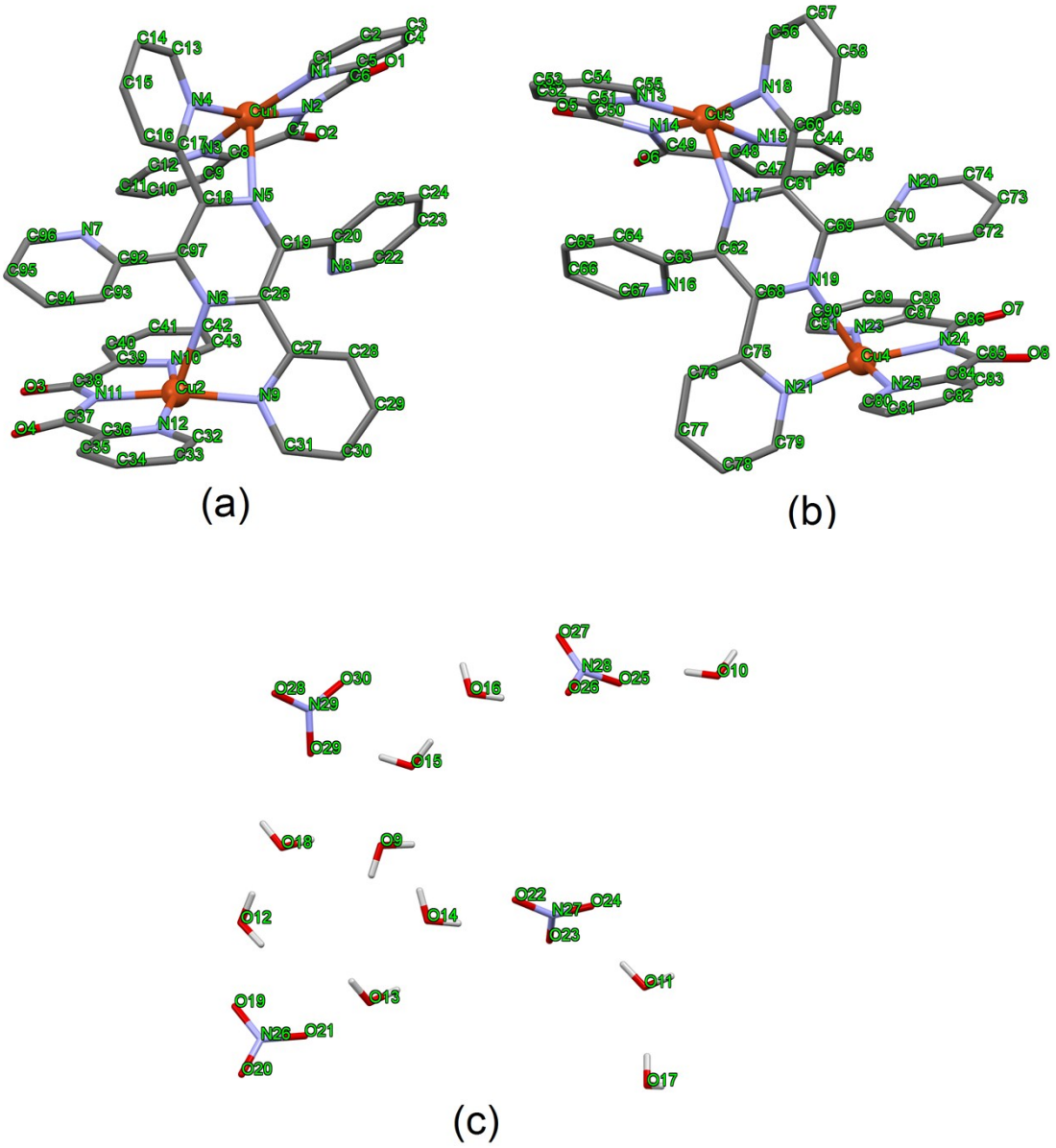

Figure S4 Perspective view of the entities that constitute the asymmetric unit of **1** with arbitrary atom and labelling. The dinuclear units containing Cu1/Cu2 (a) and Cu3/Cu4 (b) as well as the water/nitrate network (c) are depicted with independent orientation for the sake of clarity.

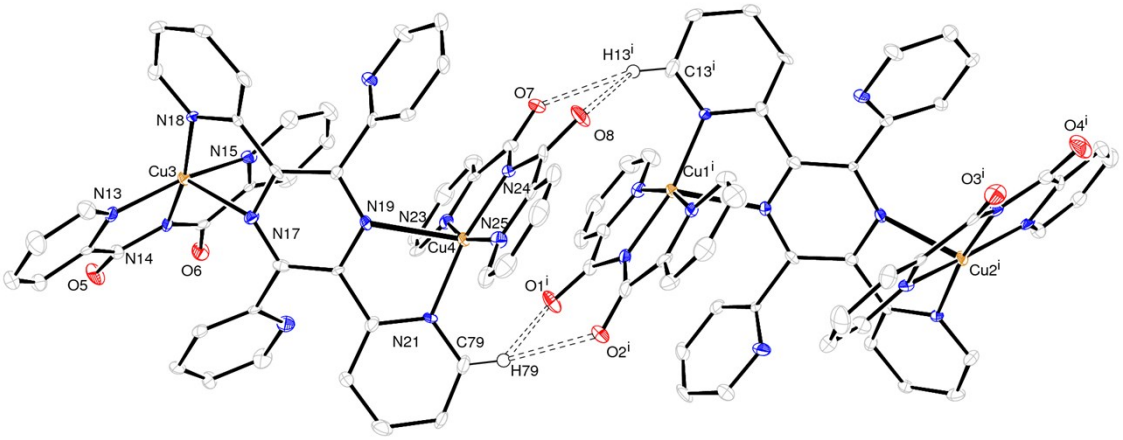

Figure S5 A perspective view of adjacent dinuclear units of **1** connected by hydrogen bonds along the [100] direction. The hydrogen atoms involved in these intermolecular bonds (double dashed lines) are represented as arbitrary radius spheres and the ellipsoids of the non-hydrogen atoms are at the 50% probability level. The remaining hydrogen atoms, water molecules of crystallization and nitrate counter ions were omitted for the sake of clarity. Symmetry code: (i) = x+1, y, z.

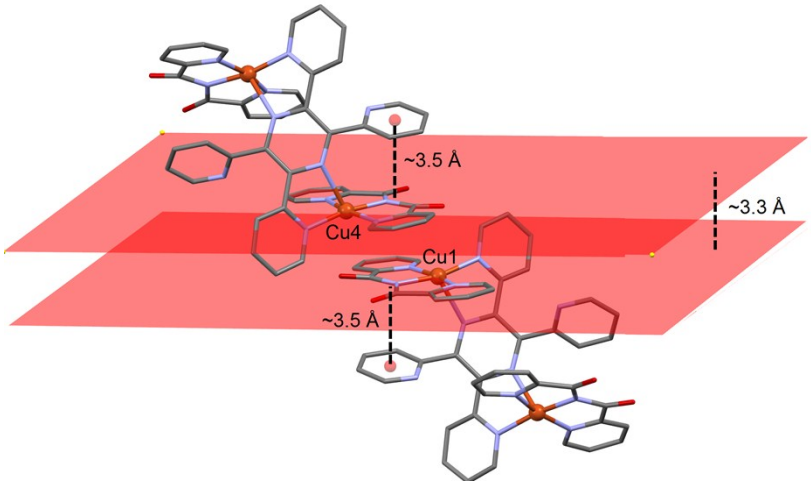

Figure S6 View of two neighbouring dinuclear units in **1** with least-squares through the copper atom and bpca groups. The distance between the least-squares and that between them and the calculated centroid of neighboring tppz-pyridyl rings are indicated. Hydrogen atoms were omitted for the sake of clarity.

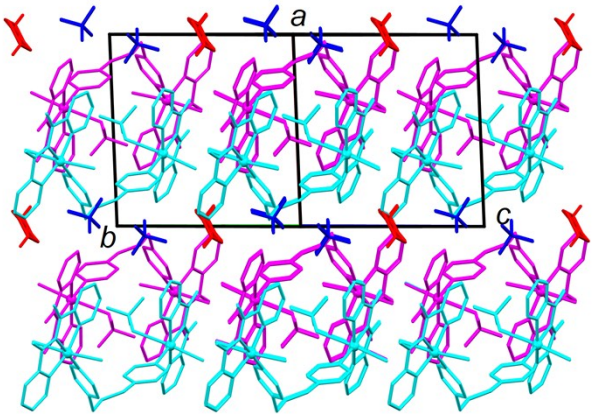

(a)

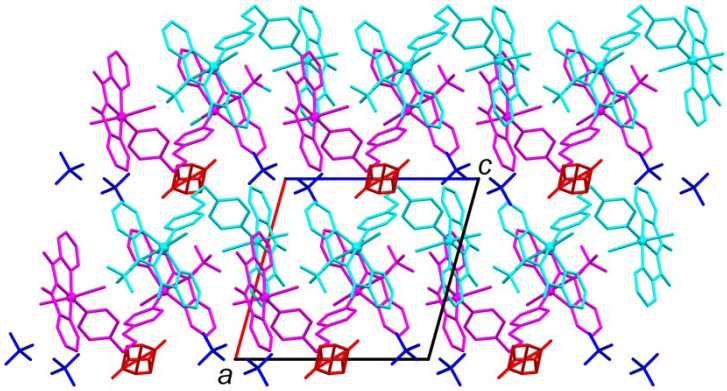

(b)

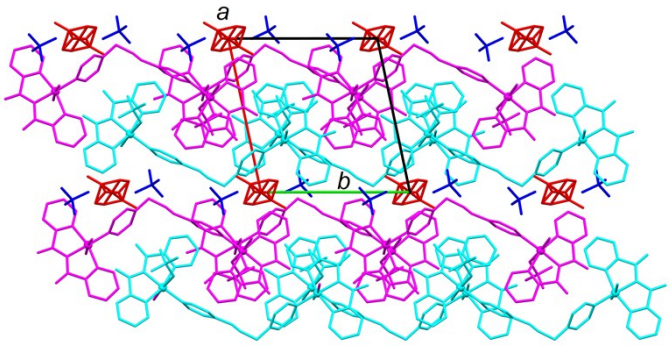

(c)

Figure S7 View of **2** showing the stacking of layers normal to the planes (a) (011), (b) (010) and (c) (001) and the channel structure filled by the disordered water molecules (in red) and one of the perchlorate counter ions (in blue). Hydrogen atoms were omitted for sake of clarity.

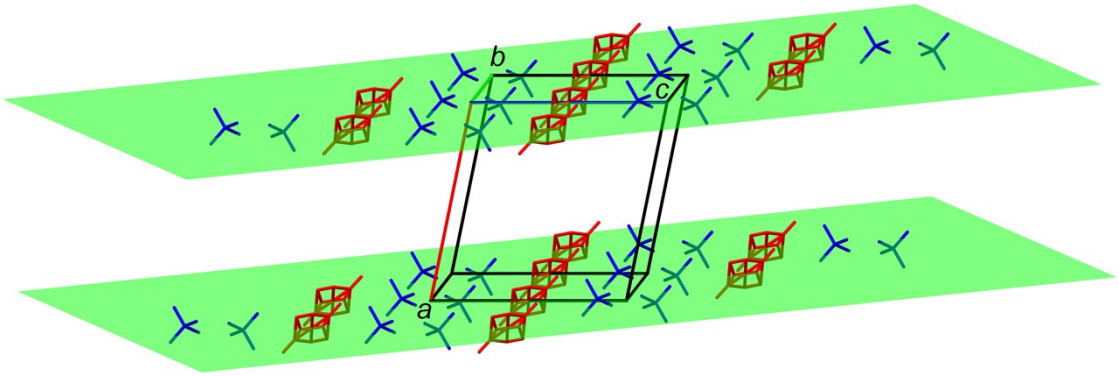

(a)

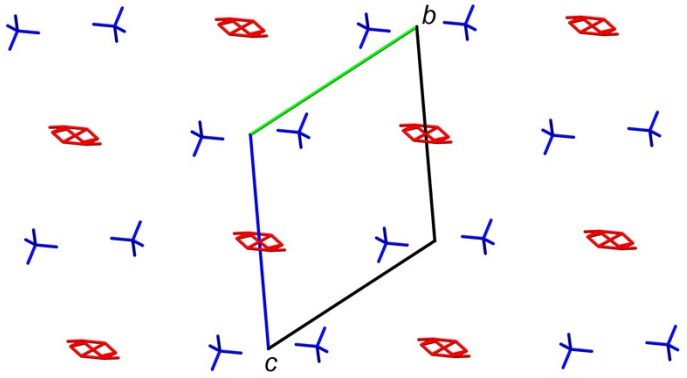

(b)

Figure S8 (a) View of **2** showing two neighbouring layers formed by disordered water molecules (moiety in red) and one of the perchlorate anions (in blue). The least-squares plane through the two layers is also shown. (b) View of the layer normal to (100) plane in **2**.

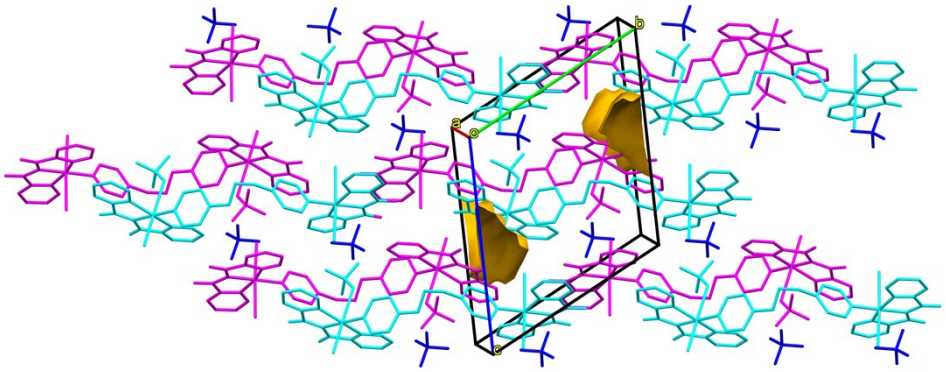

Figure S9 Packing view of **2** on the *bc* plane showing the voids (surfaces in orange) calculated by MERCURY[18] using the contact surface approach with a grid spacing and a probing-sphere radius of 0.7 and 1.1 Å, respectively. The disordered water molecules were purposely removed from the CIF file before the calculation.

Table S1 Selected bond lengths (Å) and angles (°) for [{Cu(bpca)}$_2$(μ-tppz)] $(NO_3)_2 \cdot 5H_2O\}_2$ (**1**)

Cu1–N Bonds		Cu2–N Bonds		Cu3–N Bonds		Cu4–N Bonds	
Cu1–N1	1.989(7)	Cu2–N10	2.004(4)	Cu3–N13	1.987(4)	Cu4–N19	2.330(4)
Cu1–N1	1.989(7)	Cu2–N11	1.913(5)	Cu3–N14	1.894(5)	Cu4–N21	1.961(5)
Cu1–N2	1.902(5)	Cu2–N12	1.996(4)	Cu3–N15	2.006(4)	Cu4–N23	2.013(7)
Cu1–N3	1.996(7)	Cu2–N6	2.360(5)	Cu3–N17	2.318(5)	Cu4–N24	1.902(5)
Cu1–N5	2.329(4)	Cu2–N9	1.979(6)	Cu3–N18	1.972(6)	Cu4–N25	1.991(5)
N–Cu1–N Angles		**N–Cu2–N Angles**		**N–Cu3–N Angles**		**N–Cu4–N Angles**	
N2–Cu1–N1	82.7(2)	N11–Cu2–N10	81.8(2)	N18–Cu3–N13	97.5(2)	N25–Cu4–N24	82.0(2)
N1–Cu1–N4	94.9(2)	N11–Cu2–N12	82.3(2)	N13–Cu3–N14	82.0(2)	N24–Cu4–N23	82.2(2)
N4–Cu1–N3	99.8(2)	N12–Cu2–N9	97.7(2)	N14–Cu3–N15	81.5(2)	N23–Cu4–N21	98.1(2)
N3–Cu1–N2	81.9(2)	N9–Cu2–N10	97.3(2)	N15–Cu3–N18	98.6(2)	N21–Cu4–N25	97.0(2)
N5–Cu1–N3	91.1(2)	N6–Cu2–N10	89.4(2)	N17–Cu3–N18	76.2(2)	N19–Cu4–N25	97.5(2)
N5–Cu1–N2	115.1(2)	N6–Cu2–N11	113.6(2)	N17–Cu3–N13	98.4(2)	N19–Cu4–N24	113.9(2)
N5–Cu1–N1	97.1(2)	N6–Cu2–N12	100.4(2)	N17–Cu3–N14	115.0(2)	N19–Cu4–N23	91.1(2)
N5–Cu1–N4	76.8(2)	N6–Cu2–N9	75.8(2)	N17–Cu3–N15	88.9(2)	N19–Cu4–N21	76.6(2)

Table S2 Selected bond lengths (Å) and angles (°) for [Cu(bpca)(H_2O)(ClO_4)(μ-bpp)Cu(bpca)(H_2O)$_2$]$ClO_4 \cdot H_2O$ (**2**)

Cu1–N/O Bonds		N/O–Cu1–N Angles		N/O–Cu2–N Angles	
Cu1–N1	2.012(2)	N1–Cu1–N4	99.59(9)	N7–Cu2–N8	81.43(9)
Cu1–N2	1.942(2)	N4–Cu1–N3	96.31(9)	N8–Cu2–N5	101.35(9)
Cu1–N3	2.026(2)	N3–Cu1–N2	81.89(9)	N5–Cu2–N6	95.27(9)
Cu1–N4	1.993(2)	N2–Cu1–N1	82.21(9)	N6–Cu2–N7	81.73(8)
Cu1–O14	2.674(2)	O14–Cu1–N3	84.73(8)	O5–Cu2–N7	92.03(7)
Cu1–O15	2.522(3)	O14–Cu1–N4	91.73(7)	O5–Cu2–N8	89.76(8)
Cu1–N/O Bonds		O14–Cu1–N1	89.31(7)	O5–Cu2–N5	89.57(8)
Cu2–N5	1.999(2)	O14–Cu1–N2	88.10(7)	O5–Cu2–N6	100.00(8)
Cu2–N6	2.027(2)	O15–Cu1–N3	101.15(8)	O6–Cu2–N8	89.23(9)
Cu2–N7	1.943(2)	O15–Cu1–N4	87.77(8)	O6–Cu2–N7	91.47(8)
Cu2–N8	2.033(2)	O15–Cu1–N1	85.00(8)	O6–Cu2–N6	82.04(8)
Cu2–O5	2.369(2)	O15–Cu1–N2	92.58(8)	O6–Cu2–N5	87.01(8)
Cu2–O6	2.649(3)				

Table S3 Hydrogen bonds (Å) in **1** given the donor…acceptor distances.

O9···O14	2.764(9)	O10···O28	2.786(9)	O12···O18	2.658(9)	O15···O16	2.763(8)
O9···O15	2.73(1)	O11···O17	2.769(9)	O12···O19	2.80(1)	O15···O29	2.888(7)
O9···O18	2.82(1)	O11···O20	2.86(1)	O13···O14	2.837(8)	O16···O17	2.83(1)
O10···O18	2.90(1)	O11···O23	2.98(1)	O13···O21	2.997(9)	O16···O26	2.776(8)
O10···O25	2.89(1)	O11···O24	3.024(9)	O14···O22	2.772(9)	O17···O27	2.840(9)